

This paper is a postprint of a paper submitted to and accepted for publication in IET Optoelectronics and is subject to Institution of Engineering and Technology Copyright. The copy of record is available at IET Digital Library

Performance Evaluation of Turbulence-Accentuated Interchannel Crosstalk for Hybrid Fibre and FSO WDM Systems using Digital Pulse Position Modulation

†Afamefuna M. Mbah, John G. Walker, Andrew J. Phillips

Division of Electrical Systems and Optics, Faculty of Engineering, University of Nottingham, University Park, Nottingham NG7 2RD, UK

†Corresponding author's email: eexammb@nottingham.ac.uk

Tel: +44 (0) 7574928581, Fax: +44 (0) 115 951 5616

Abstract

A hybrid fibre and free space optical (FSO) communication link using digital pulse position modulation (DPPM) in a wavelength division multiplexing (WDM) system is proposed. Such a system, which could provide a power efficient, robust and flexible solution to high speed access networks, is a contender for a passive optical network (PON) solution and could readily be deployed in areas with restrictions in optical fibre installation, or alternatively as a disaster recovery network. However, the effects of interchannel crosstalk, which is common in WDM systems, and atmospheric turbulence-induced scintillation, limit the performance of such system. Both impairments, which could combine in some cases to further degrade the system performance, are investigated here. Specifically, the symbol error probability, the required optical transmission power and power penalties are derived. Furthermore, the required performance of the demultiplexers in terms of adjacent channel rejection is studied with respect to the FSO link length. A simple relationship between the turbulence attenuation and crosstalk

is derived to facilitate demultiplexer selection in the design and analysis of practical systems without forward error correction (FEC) coding. Results also show that DPPM systems are more power efficient than OOK systems in the presence of crosstalk accentuated by atmospheric turbulence.

1 Introduction

The optical fibre transmission spectrum provides huge and unregulated bandwidth immune from electromagnetic interference, with low signal attenuation around the 1550 nm wavelength region [1], and is the medium of choice for high speed access networks. Optical fibre technology is well developed in access networks, and can potentially support high speed transmission to users in their homes and offices [2]. Thus optical fibre is commonly found in optical interconnects, point-to-point links between local area networks (LANs) and within passive optical networks (PONs) [3-5], and is easily compatible with most multiplexing/multiple access techniques. Other benefits of fibre networks include low signal attenuation and low cost compared to the previously used twisted-pair copper cables found in digital subscriber loop systems [1, 6]. In some cases however, it may not be possible to lay fibre due to infrastructural barriers or for environmental reasons [7], or due to a need for rapid deployment, and an alternative optical communication network may be required.

In many cases free space optical (FSO) communication links are easier and cheaper to deploy than optical fibre links [2, 8]. FSO communication systems have been widely applied in inter-satellite and deep space communications and have recently received more interest in terrestrial communication with specific applications such as pre-deployed back up link, rapidly deployed disaster recovery link and enterprise connectivity e.g. LANs and wide area networks (WANs) [2, 4, 8]. Such systems provide extra flexibility and relative ease of upgrade as the user need

changes, and have increasingly been proposed as promising solutions to high speed transmission in the last mile of optical access networks [9]. FSO communication however requires line of sight between transceivers and, for terrestrial (atmospheric) application, system performance is adversely affected by attenuation (due to atmospheric particles), beam spreading and turbulence-induced scintillation [10-13].

Wavelength division multiplexing (WDM) has application in both optical fibre and FSO systems [1, 2, 4]. With WDM PON, fixed wavelengths are assigned to each optical network unit (ONU), thus more fully exploiting the high transmission bandwidth available in the optical domain and avoiding the synchronisation and threshold acquisition required in the burst mode upstream of time division multiplexing/time division multiple access (TDM/TDMA) systems [14, 15]. Compared to TDM/TDMA PONs, WDM PON systems offer other advantages to the users such as low loss, greater security and longer reach, and are increasingly being considered as the primary solution to the continuous rise in bandwidth demand in access networks [16, 17]. In contrast to space division multiplexing (SDM), WDM supports network resource sharing, which generally reduces implementation cost. Furthermore, unlike TDM and CDM where the system bit rate and chip rate may be higher than the end user's data rate, WDM systems enable simultaneous transmission by all users at full system bit rate only limited by the electronic processing speed [1].

Digital pulse position modulation (DPPM) has successfully been applied in fibre, intersatellite and deep space optical communication systems and is a strong contender for terrestrial FSO systems [18, 19]. Several studies on FSO systems show that digital pulse modulation schemes are more power efficient schemes compared to on-off-keying (OOK) and are well suited for FSO communication systems where dispersion is negligible [11, 20-22]. Although when compared to DPPM, anisochronous digital pulse modulation schemes like DPIM and DH-PIM offer improved bandwidth efficiency and synchronisation, DPPM offers a better average

optical power requirement efficiency which is necessary in complying with eye safety limitations [22], and also provides better error rate performance [21]. Furthermore, at lower coding level (for example at coding level of 2 or 1), DPPM bandwidth efficiency is comparable to that of other digital pulse modulation schemes as shown by results in [22]. Consequently, DPPM has been considered for use in WDM systems in [23, 24], and for PON systems in [15], but would have a better application in coarse WDM systems where the additional bandwidth expansion is less problematic.

Interchannel crosstalk in a WDM DPPM system was considered in [25] for a non-turbulent channel. A hybrid fibre and FSO WDM system using DPPM, possibly presents a more feasible solution in some scenarios to high bandwidth users than a fibre or FSO only system. Such a system combines the numerous advantages of both fibre and free space optical communication with digital pulse position modulation and wavelength division multiplexing techniques and is analysed for the first time in this paper. Modelling the hybrid fibre and FSO WDM DPPM system is non-trivial; the combined effect of the different impairments on system performance is complex. Particularly, the random fluctuations in both signal and crosstalk powers due to turbulence under various DPPM coding levels could lead to high power penalties.

2 Network Structure

The network components as shown in Fig. 1 include a transmitter module which comprises of a laser driver (LD) and laser for optical signal generation, the input message signal (data) and a PPM modulator (PPM Mod) and a receiver module made up of a photodetector (PD), electrical amplifier and filter (EA) and the integrate and compare circuitry (ICC) for system decision. Thus the system is intensity modulated and the signal is received by direct detection. The downstream collecting lens may include an optical bandpass filter (OBPF) (shown in Fig.

1d) to limit background ambient light, while the demultiplexer (demux) inherently performs the optical bandpass filtering in the upstream direction. With DPPM, the system does not require dynamic tracking of a threshold unlike for some OOK systems [26], and it could exist in a PON configuration and possibly include an optical amplifier (OA) to improve the receiver sensitivity and extend the network reach [15]. The optical line terminator (OLT) is linked to a remote node (RN) via a feeder fibre and optical signals are distributed to the various optical network units (ONUs) through a turbulent free space channel. An automatic pointing and tracking system including a transmitting lens and focusable collimators or beam expanders [27] is used to launch the light exiting from the fibre end at the remote node or the transmitter at the ONU to free space. By using an automatic tracking and pointing subsystem, a narrow transmit divergence angle is achieved through adjusting the position and focal lengths of the lenses [27, 28]. The signals are received via a collimator with collecting lens at the opposite end. The collecting lenses are assumed to be widely spaced but appropriately orientated and aligned with the respective transmitting lenses such that signal from one wavelength is not received at another wavelength through the wrong collecting lens. In this way, it is easy to avoid intrachannel crosstalk. The optical amplifier, downstream demultiplexer (demux) and upstream multiplexer (mux) are conveniently located at a remote node, while the upstream demux and downstream mux are located at the OLT. This choice for the OA position limits the possibility of fibre non-linear effects occurring during the downstream transmission since the signal would not be boosted before going into the fibre.

Interchannel crosstalk occurs due to the imperfect nature of the demux (in the OLT for upstream transmission or the remote node for downstream transmission). Additionally, turbulence puts more stringent demands on the rejection of non-signal wavelengths by the demux (as a mean signal-to-crosstalk ratio of e.g. 25 dB could vary widely above and below that value due to the independence of turbulence on signal and crosstalk paths). However in

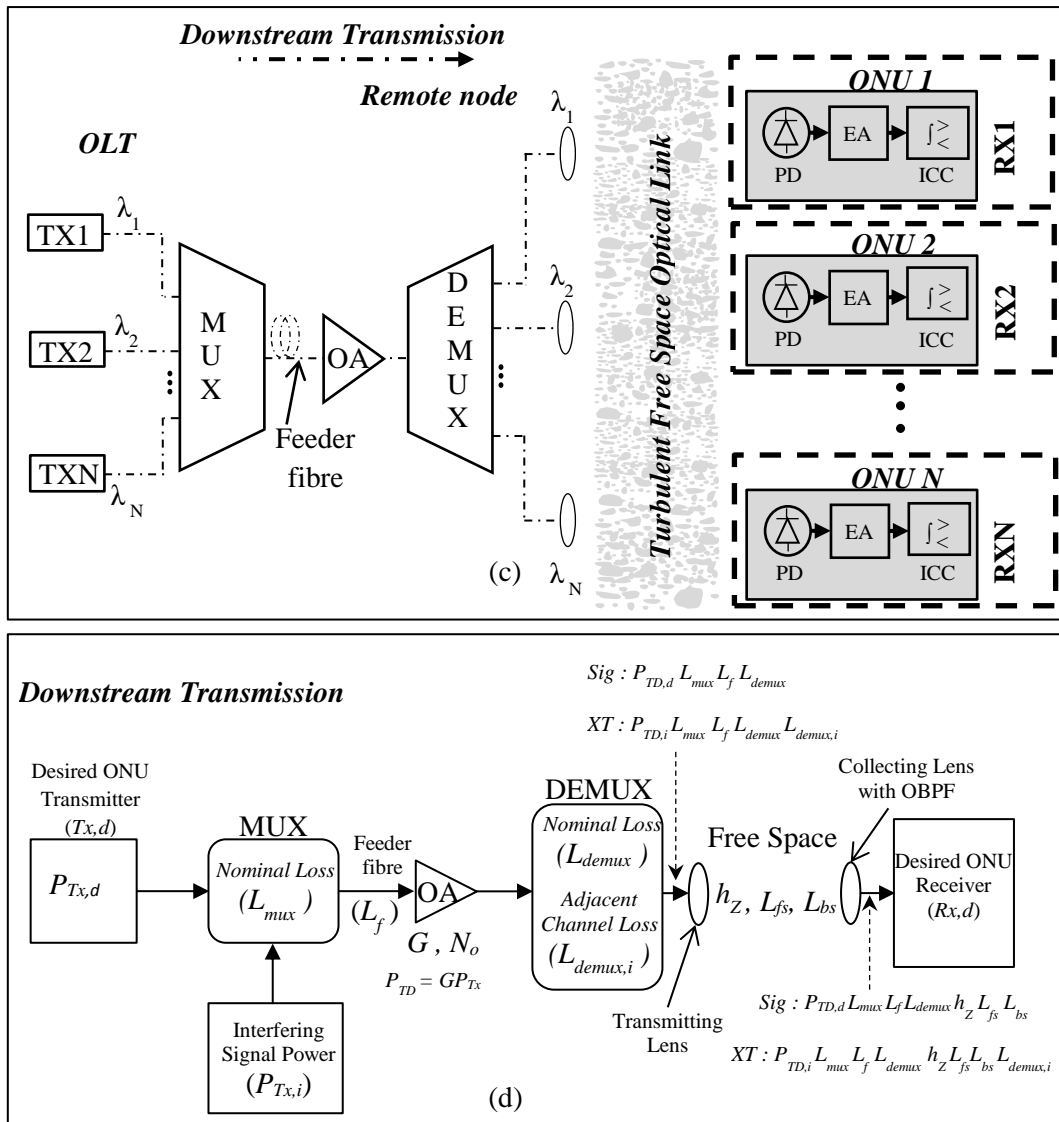


Fig. 1 Optically Preamplified WDM DPPM Network: (a) Upstream system diagram (b) Upstream functional diagram (c) Downstream system diagram and (d) Downstream functional diagram

3 Turbulence Channel Modelling

The effects of turbulence are characterized using the gamma-gamma (GG) probability density function (pdf), which is given as [10, 13, 29]

$$p_{GG}(h_z) = \frac{2(\alpha\beta)^{(\alpha+\beta)/2}}{\Gamma(\alpha)\Gamma(\beta)} h_z^{((\alpha+\beta)/2)-1} K_{\alpha-\beta}(2\sqrt{\alpha\beta} h_z); \quad h_z > 0 \quad (1)$$

where $h_z = h_d$ or h_i is the attenuation due to atmospheric turbulence for the desired signal or interferer respectively, α is the effective number of large-scale eddies of the scattering process, β is the effective number of small-scale eddies of the scattering process, $K_n(\bullet)$ represents the modified Bessel function of the second kind, order n and $\Gamma(\bullet)$ is the gamma function. The Rytov variance σ_R^2 distinguishes the various link turbulence regimes (weak turbulence (WT) $\sigma_R^2 < 1$, moderate turbulence (MT) $\sigma_R^2 \approx 1$, strong turbulence (ST) $\sigma_R^2 > 1$ and saturated turbulence $\sigma_R^2 \rightarrow \infty$), and is given by [10, 29]

$$\sigma_R^2 = 1.23 C_n^2 k^{7/6} l_{fso}^{11/6} \quad (2)$$

where C_n^2 is the refractive index structure constant, typically ranging from $\approx 10^{-17} m^{-2/3}$ to $\approx 10^{-13} m^{-2/3}$, $k = 2\pi/\lambda$ is the optical wave number, λ is the optical wavelength and l_{fso} is the free space link length [10, 13].

For plane wave propagation, the α and β parameters incorporating aperture averaging are respectively written as [10, 13, 29]

$$\alpha = \left\{ \exp \left[\frac{0.49 \sigma_R^2}{\left(1 + 0.65 d^2 + 1.11 \sigma_R^{12/5}\right)^{7/6}} \right] - 1 \right\}^{-1} \quad (3)$$

$$\beta = \left\{ \exp \left[\frac{0.51 \sigma_R^2 \left(1 + 0.69 \sigma_R^{12/5}\right)^{-5/6}}{1 + 0.9 d^2 + 0.62 d^2 \sigma_R^{12/5}} \right] - 1 \right\}^{-1} \quad (4)$$

where $d = \sqrt{k D_{RX}^2 / 4 l_{fso}}$ is the normalized receiver collecting lens (RCL) radius and D_{RX} is the RCL diameter. The turbulence induced scintillation of the desired signal and interferer are each treated independently for the upstream as each is transmitted over different free space path,

however, for the downstream transmission, both signal and interferer exit the same RCL and travel over the same physical path.

The fibre loss is $L_f = 10^{(-\alpha_f l_f)/10}$ and the free space loss is $L_{fs} = 10^{(-\alpha_{fs} l_{fs})/10}$ where α_f and α_{fs} are the attenuation coefficients of fibre and free space respectively (in dB/km), and l_f is the fibre link length (in km). The nominal demux loss L_{demux} /multiplexer (mux) loss L_{mux} is about 3 dB [5, 30], while the interferer's demux loss $L_{demux,i}$ is the additional loss that interferer experiences upon coupling to the desired signal wavelength port, and also defines the signal to crosstalk ratio (in the situation when the input signal and crosstalk power are equal). The free space transmission beam spreading loss in dB for a small transmitter aperture in the presence of turbulence is written as [10, 13, 27].

$$L_{bs} = 20 \log_{10} \left(\frac{D_{RX}}{D_e} \right) \quad (5)$$

where D_e is the beam diameter at the collecting lens due to diffraction and turbulence written as,

$$D_e = d_l \left[1 + 1.33 \sigma_R^2 \left(\frac{2l_{fs}}{k(d_l/2)^2} \right)^{5/6} \right]^{1/2} \quad (6)$$

$d_l = \varphi_{TX} l_{fs}$ [13, 27] defines the beam diameter due to diffraction only and φ_{TX} represents the transmitter divergence angle for either the desired or interfering signal.

A coupling loss is encountered at the interface between the free space link and the fibre link. Assuming that the fibre ends connected to the multiplexers are within the RCL focal plane, the coupling efficiency η_c is given by [31]

$$\eta_c = 8a^2 \int_0^1 \int_0^1 \left(\exp \left[- \left(a^2 + \frac{A_{RX}}{A_c} \right) (x_1^2 + x_2^2) \right] I_0 \left(2 \frac{A_{RX}}{A_c} x_1 x_2 \right) x_1 x_2 \right) dx_1 dx_2 \quad (7)$$

where $a = 1.12$ is the coupling geometry parameter, expressed as the ratio of the RCL radius to the back-propagated fibre mode radius, and optimum for a fully coherent incident plane wave in the absence of turbulence [31], $A_{RX} = \pi D_{RX}^2 / 4$ is the RCL area, $A_c = \pi \rho_c^2$ is the spatial coherence area of the incident wave, with radius $\rho_c = (1.46 C_n^2 k^2 I_{fs})^{-3/5}$, $I_0(\bullet)$ is a modified Bessel function of the first kind, order zero.

4 DPPM Crosstalk Modelling

A DPPM frame consists of $n = 2^M$ equal time slots of duration $t_s = M / nR_b$, where M is the coding level and R_b is the data rate. For example, at binary data rate of 2.5 Gbps, the DPPM frames shown in Fig. 2 for $M = 2$ contain four slots each and thus the pulse in each frame represents a 2-bit word transmitted at slot rate of 5 GHz. In WDM DPPM systems, the bandwidth expands with increasing coding level and appropriate spacing is required between the wavelengths for systems with high coding level. At $M = 2$, the bandwidth expansion of the system is minimum, therefore this analysis is performed at $M = 2$ which represents a practical trade-off.

For analytical convenience, assuming that only slots of crosstalk and signal align during reception, there is the possibility for the crosstalk frame to misalign with the signal frame by 1, 2 or 3 slots, or to fully align with the signal frame (i.e. $n_1 = 1, 2, 3$ or 0 as shown in Fig. 2). Thus during signal frame reception, the interfering signal frame is also being received either in full alignment with the signal frame or misaligned by 1, 2 or 3 slots. And, although there is only one pulse in the interfering signal frame, the desired signal may be impaired by zero (Fig. 2, $n_1 = 1$), one (Fig. 2, $n_1 = 0$ and 2) or two (Fig. 2, $n_1 = 3$) crosstalk pulses depending on the position of the pulse in the interfering signal frame and the pattern of (mis)alignment with the desired signal frame. This condition which neglects partial slot misalignment was referred to

as only slots aligned (OSA) in [25], and leads to a quick approach which predicts sensible results for both single and multiple crosstalk sources.

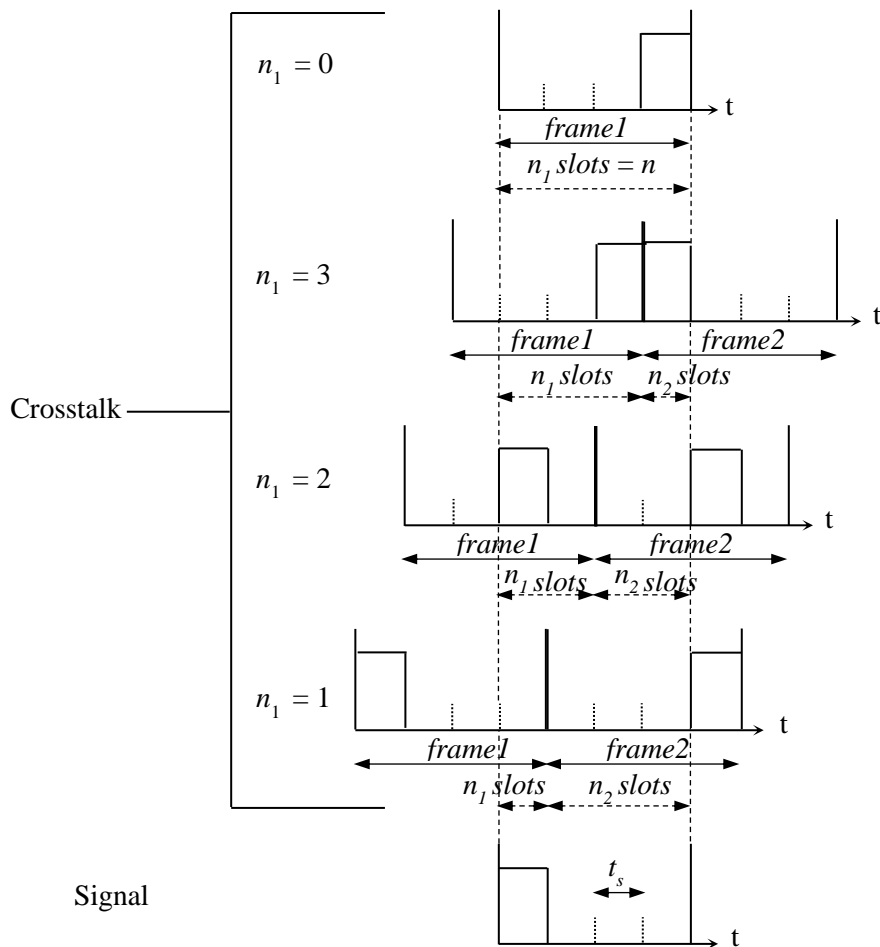


Fig. 2 Illustration of different frame misalignments between crosstalk and signal in DPPM WDM FSO receiver with $M = 2$, ($n_1 = 1, 2, 3$ and 0 are optional misalignment forms)

A practical WDM system consists of many wavelengths, and signals in all active wavelengths contribute some amount of crosstalk to signals on other wavelengths. The effects of crosstalk from adjacent wavelengths are typically more severe than crosstalk from other wavelengths further separated from the desired wavelength. Therefore, for immediate insight into a WDM DPPM system, the simple case of a single adjacent interferer is considered in this work.

However, the analysis is useful wherever we have the possibility of turbulence-accentuated crosstalk. A typical scenario where the single interferer model could be applied is in a system where one interferer is much nearer to the remote node compared to the other interferers. In such case, there is significant asymmetry in crosstalk power of the interferers and the single dominant interferer could be used for the system performance calculations. In addition, since the effect of a single interferer with high power is worse than that of many interferers with equivalent power [25], multiple interfering signals could be lumped into a single wavelength and equivalently modelled as a single crosstalk to present the worst case performance.

For the upstream transmission, the received DPPM rectangular pulse power at the photodetector input for the desired signal and the interferer are respectively written as

$$P_d(h_d) = P_{TU,d} h_d L_{fs,d} L_{bs,d} \eta_{c,d} L_{mux} L_f L_{demux} \quad (8)$$

$$P_i(h_i) = P_{TU,i} h_i L_{fs,i} L_{bs,i} \eta_{c,i} L_{mux} L_f L_{demux} L_{demux,i} \quad (9)$$

and the single polarisation ASE power spectral density (PSD) at the photodetector input for the desired signal and the interferer are respectively written as

$$N_{o,d} = 0.5(NFG - 1)h \nu L_f L_{demux} \quad (10)$$

$$N_{o,i} = 0.5(NFG - 1)h \nu_i L_f L_{demux} L_{demux,i} \quad (11)$$

where G and NF are the optical amplifier gain and noise figure respectively, h is Planck's constant, ν and ν_i are the optical frequencies of the desired signal and interferer respectively.

Also, for the downstream transmission, the received DPPM rectangular pulse power for the desired signal and the interferer are respectively written as

$$P_d(h_z) = P_{TD,d} h_z L_{mux} L_f L_{demux} L_{fs} L_{bs} \quad (12)$$

$$P_i(h_z) = P_{TD,i} h_z L_{mux} L_f L_{demux} L_{demux,i} L_{fs} L_{bs} \quad (13)$$

and the single polarisation ASE PSD at the photodetector input for the desired signal and the interferer are respectively written as

$$N_o = 0.5(NFG - 1)h\nu L_{demux} L_{fs} L_{bs} \quad (14)$$

$$N_{o,i} = 0.5(NFG - 1)h\nu_i L_{demux} L_{demux,i} L_{fs} L_{bs} \quad (15)$$

Following [11, 18, 25], the general equations for the upstream transmission are derived below in (16) - (20), the equations for the downstream are recovered by replacing the attenuation due to atmospheric turbulence for the desired signal/interferer (h_d, h_i) with h_z .

The means and variances of the random variables both representing the integration over the slot that contains only the signal pulse, only crosstalk pulse, both signal and crosstalk pulses and no pulses (i.e. empty slot) are derived and respectively written as:

$$\mu_{X_{sig,int}}(h_d, h_i) = \frac{LRqN_o}{t_s} + Gq (sigRP_d(h_d) + intR_i P_i(h_i)) \quad (16)$$

$$\sigma_{X_{sig,int}}^2(h_d, h_i) = \sigma_{th}^2 + \left(\frac{LRq^2 N_o (1 + RN_o)}{t_s^2} \right) + Gq^2 \left[\left(R + 2R^2 N_o \right) \frac{sigP_d(h_d)}{t_s} + \left(R_i + 2R_i^2 N_{o,i} \right) \frac{intP_i(h_i)}{t_s} \right] \quad (17)$$

where $sig/int = 0$ or 1 depending on the presence of signal/crosstalk pulse in the slot or not, σ_{th}^2 is the DPPM thermal noise variance, $R = \eta/h\nu$, $R_i = \eta/h\nu_i$, η is the photodetector quantum efficiency, q is the electron charge, $L = B_o m_t t_s$ is the product of spatial and temporal modes [11], B_o is the demux or optical bandpass filter (OBPF) channel bandwidth and m_t is the number of ASE noise polarisation states. The means and variances have been derived with modifications to account for crosstalk–ASE beat noise assuming the interferer and the desired signal experiences the same ASE noise at the amplifier output [32].

Given that each symbol has equal probability of being transmitted in a slot, the probability that a symbol is successfully received in the presence of crosstalk and atmospheric turbulence

$P_{ws(l,r)}(h_d, h_i) = 1 - P_{we(l,r)}(h_d, h_i)$ where $P_{we(l,r)}(h_d, h_i)$ is the symbol error probability in the presence of crosstalk and turbulence, $l \in \{0,1,2\}$ and $r \in \{0,1\}$ denote the number of crosstalk occurring in the signal frame and signal pulse slot respectively. Following the same treatment as [25], one can write that:

$$P_{ws(l,r)}(h_d, h_i) \geq \prod_{\substack{j=1 \\ j \neq \text{sig slot}}}^n P(X_{1,\text{int}} > X_j | h_d, h_i) \quad (18)$$

where X_j represents the content of the non-signal slot $X_{0,\text{int}}$, and

$$P_{we(l,r)}(h_d, h_i) \leq 1 - (1 - P(X_{0,0} > X_{1,\text{int}} | h_d, h_i))^{n-1-(l-r)} (1 - P(X_{0,1} > X_{1,\text{int}} | h_d, h_i))^{l-r} \quad (19)$$

Assuming that the random variables $X_{1,\text{int}}$ and $X_{0,\text{int}}$ are Gaussian, the expression

$P(X_{0,\text{int}} > X_{1,\text{int}} | h_d, h_i)$ using the GA, is of the general form [11, 25]

$$P(X_{0,\text{int}} > X_{1,\text{int}} | h_d, h_i) = 0.5 \operatorname{erfc} \left(\frac{\mu_{X_{1,\text{int}}}(h_d, h_i) - \mu_{X_{0,\text{int}}}(h_d, h_i)}{\sqrt{2(\sigma_{X_{1,\text{int}}}^2(h_d, h_i) + \sigma_{X_{0,\text{int}}}^2(h_d, h_i))}} \right) \quad (20)$$

5 BER Analysis

In a WDM DPPM system with a single interferer, there may be no crosstalk pulse in the signal frame (for example, compare the signal frame in Fig. 2 with the crosstalk frame when $n_1 = 1$). Furthermore, one or two crosstalk pulse(s) may possibly impair the signal frame (compare the signal frame in Fig. 2 with the crosstalk frame when $n_1 = 2$ or 3). However, only one crosstalk pulse can hit a single slot in the signal frame.

The BERs conditional on turbulence and crosstalk frame overlap (n_1) for the upstream and downstream are respectively written as

$$BER_{U_i}(h_d, h_i, n_1) = p_{f(l)}(n_1) \frac{n}{2(n-1)} (p_{s(l)}(1) P_{we(l,1)}(h_d, h_i) + p_{s(l)}(0) P_{we(l,0)}(h_d, h_i)) \quad (21)$$

and

$$BER_{D_i}(h_Z, n_1) = p_{f(l)}(n_1) \frac{n}{2(n-1)} (p_{s(l)}(1)P_{we(l,1)}(h_Z) + p_{s(l)}(0)P_{we(l,0)}(h_Z)) \quad (22)$$

where $p_{f(l)}(n_1)$ denote the probability of l crosstalk pulses hitting the signal frame (calculated the same as in [25]), and n_1 is the number of slots in crosstalk frame 1 that overlap the signal frame. Also $p_{s(l)}(r)$ denote the probability of r out of l crosstalk pulses hitting the signal slot so that the probability that a crosstalk pulse hits the signal pulse slot $p_{s(l)}(1) = l/n$ and the probability that crosstalk pulse(s) hit an (unspecified) empty slot $p_{s(l)}(0) = (n-l)/n$. The no crosstalk symbol error probability $P_{we(0,0)}(h_d)$ is treated the same as in [25], $P_{we(l,1)}(h_d, h_i)$ and $P_{we(l,0)}(h_d, h_i)$ are calculated using (19) for $r = 1$ and 0 respectively, and represent word error contributions when the interferer and the desired signal have experienced turbulence from different (i.e. assumed independent) atmospheric links as in the upstream. Both $P_{we(l,1)}(h_Z)$ and $P_{we(l,0)}(h_Z)$ are calculated using (19) for $h_d \approx h_i \approx h_Z$ (i.e. where the interferer and the desired signal have travelled the same turbulence path like in the downstream), and for $r = 1$ and 0 respectively.

The overall BER in the presence of crosstalk and turbulence for the upstream is thus calculated by summing up all the error contribution calculated from (21) for all values of l and averaging over all values of crosstalk frame overlap (n_1) and both the turbulence pdfs for the desired signal and the interferer. It is written as

$$\overline{BER}_U = \int_0^\infty \int_0^\infty \frac{1}{n} \sum_{n_1=0}^{n-1} \sum_{l=0}^2 BER_{U_l}(h_d, h_i, n_1) p_{GG,d}(h_d) p_{GG,i}(h_i) dh_d dh_i \quad (23)$$

Also the overall BER in the presence of crosstalk and turbulence for the downstream is calculated by summing up all the error contribution calculated from (22) for all values of l and

averaging over all values of n_1 and the turbulence pdfs for only the desired signal. It is written as

$$\overline{BER}_D = \int_0^\infty \frac{1}{n} \sum_{n_1=0}^{n-1} \sum_{l=0}^2 BER_{D_l}(h_Z, n_1) P_{GG,d}(h_Z) dh_Z \quad (24)$$

For fixed misalignment of crosstalk and signal frames, (23) and (24) are modified to exclude the requirement for averaging over all values of n_1 , and then calculated for the value of n_1 that correspond to the fixed misalignment.

6 Results and Discussion

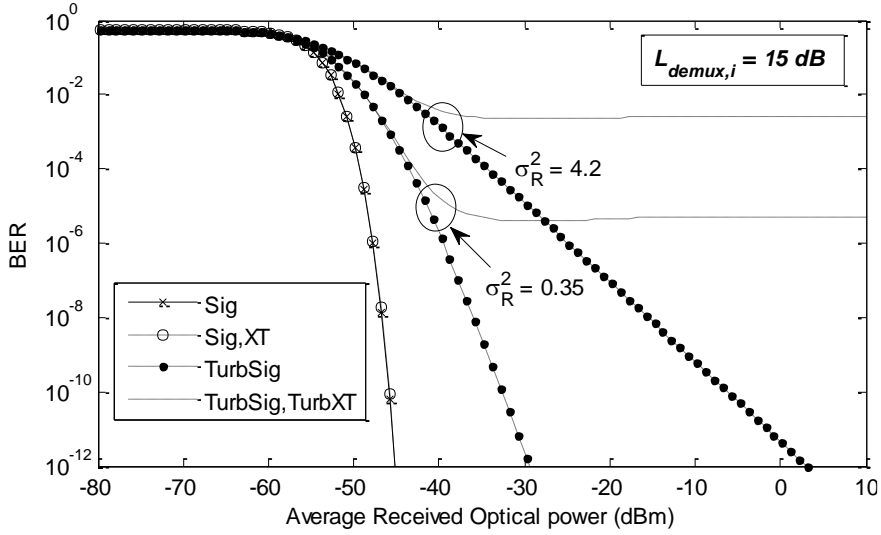
Bit error rate (BER), required optical transmission power and power penalty results are presented using parameters reported in Table 1. The DPPM coding level $M = 2$ is used for all calculations to keep the bandwidth expansion low while still maintaining the attractive features of DPPM. The required optical power referred to in this work represents the transmitter power at the OLT (for downstream transmission) and ONU (for upstream transmission). A transmission power of 20 dBm is considered safe for free space transmission around the 1550 nm wavelength region [33]. Refractive index structure constant ranging from $C_n^2 = 10^{-16} \text{ m}^{-2/3}$ to $10^{-13} \text{ m}^{-2/3}$ are used for free space optical link length of 200 m to 2000 m, corresponding to Rytov variance (σ_R^2) range of 1.04×10^{-4} to 7.10 and covering all the turbulence regimes. Aperture averaging is incorporated in the turbulence model for scintillation mitigation through the use of (3) and (4). Amplifier saturation based effects, fibre dispersion and other nonlinearities are neglected in the analysis, and a perfect extinction ratio is assumed for the OOK calculations. The thermal noise variance is back calculated using the DPPM bandwidth expansion factor $B_{\text{exp}} = 2^M / M$ [34], such that $\sigma_{th-DPPM}^2 = B_{\text{exp}} \sigma_{th-OOK}^2$ and $\sigma_{th-OOK} = 7 \times 10^{-7} \text{ A}$ is obtained from a model of a PIN receiver with $R_b = 2.5 \text{ Gbps}$ at BER of 10^{-12} assuming a sensitivity of -23 dBm [6]. Background ambient light power is considered negligible for a

receiver using small area collecting lens with small field of view and narrow optical noise bandwidth, and operating at 1550 nm [35]. The mux/demux channel bandwidth is assumed to be 76 GHz, with insertion loss of about 3.5 dB and adjacent channel spacing of 100 GHz in the C-band of the ITU (International Telecommunication Union) grid specification. Demux adjacent channel rejection values typically ≤ -15 dB and ≥ -45 dB have been demonstrated experimentally in [36-38] and are considered. As seen in [25], the impact of a single high power crosstalk is worse than that of many crosstalk of equivalent power. Thus in this work, a single crosstalk source from a dominant interferer is studied.

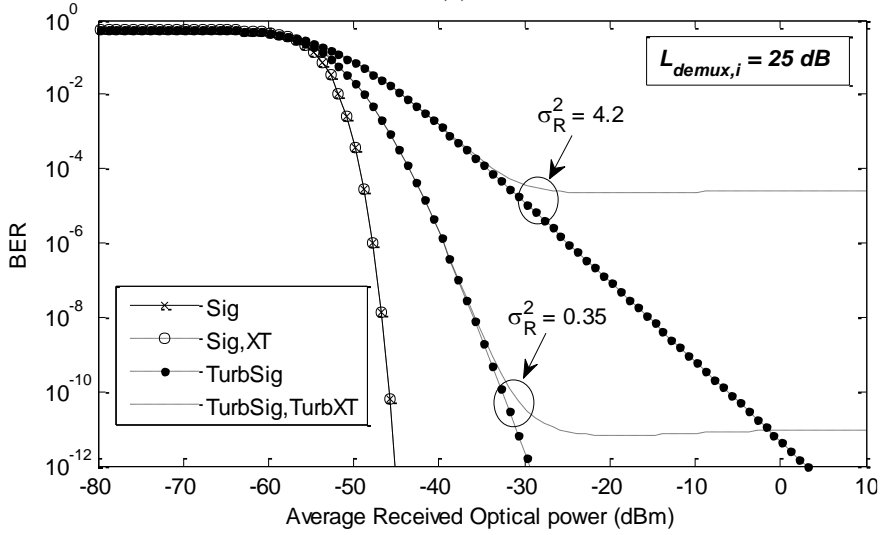
Table 1: Physical parameters used for calculations

Parameters	Description	Value
R_b	Binary data rate	2.5 Gbps
B_o	Demux or OBPF channel bandwidth	76 GHz
λ_{sig}	Desired signal wavelength	1550 nm
φ_{TX}	Transmission divergence angle	0.2 mrad
D_{RX}	Receiver collecting lens diameter	13 mm [39]
η	Receiver quantum efficiency	0.8
l_f	Feeder fibre link length	20 km
l_{fs}	Maximum free space link length	2 km
α_f	Fibre attenuation	0.2 dB/km
α_{fs}	Free space attenuation (clear air)	0.2 dB/km
G	Optical preamplifier gain	30 dB
NF	Optical preamplifier noise figure	4.77 dB
m_t	ASE noise polarisation states	2
L_{demux}	Signal demux/mux loss	3.5 dB [5, 30]

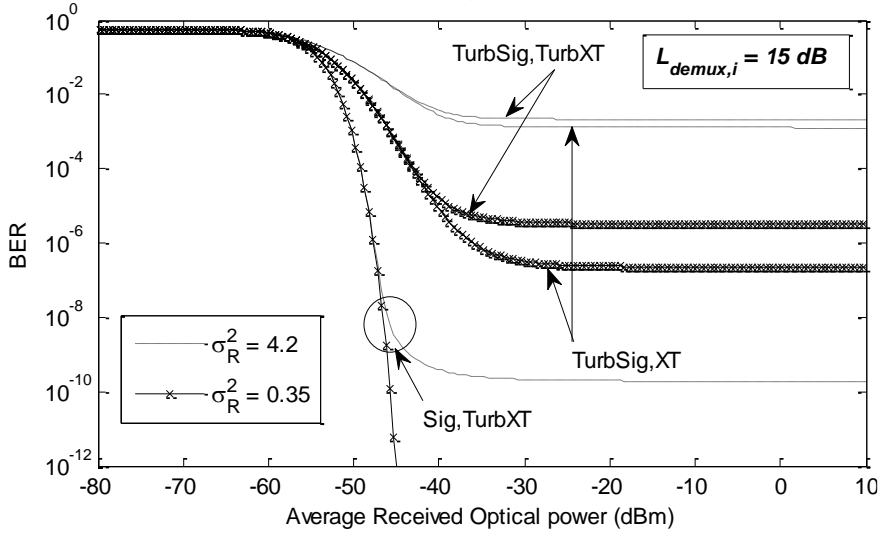
The upstream BER curves for a single interferer at both strong and weak turbulence are shown in Fig. 3 for signal and interferer FSO link length of 1500 m. For this particular result, we considered an optically preamplified receiver without any other losses, to clearly show the effects of crosstalk alone, turbulence alone and turbulent crosstalk. The Rytov variance (σ_R^2) is fixed for a particular curve and the transmitter power for the signal and interferer are assumed to be the same so only the demux adjacent crosstalk rejection loss ($L_{demux, i}$) is responsible for the crosstalk. The crosstalk effect is seen to be small without turbulence even for a demux with poor adjacent channel rejection (15 dB). However in the presence of turbulence, either for the signal or for the interferer or both, the crosstalk effect is more prominent and results in error floor as seen in Fig. 3c. The error floor occurred at a much lower BER (not shown for $\sigma_R^2 = 0.35$) for non-turbulent signal with turbulent interferer (*Sig, TurbXT*) because the power of the turbulent interferer is reduced by the demux channel rejection ratio.



(a)



(b)



(c)

Fig. 3. Upstream BER versus Average Received Optical Power (dBm) for ST and WT with σ_R^2 fixed for each curve: (a) $L_{demux,i} = 15$ dB (b) $L_{demux,i} = 25$ dB and (c) $L_{demux,i} = 15$ dB

As a result of the random fluctuation in received irradiance, atmospheric turbulence can increase or decrease the value of the desired signal or interferer pulse at decision time. Therefore, the error floor occurs when turbulence has increased the interfering signal (and hence the crosstalk power) value in the empty slot or attenuated the desired signal pulse value in the signal slot, to a sufficiently significant extent. This happens at high signal power when the effect of (other) noise on the system is negligible. To understand it properly firstly consider the extreme situation of a noiseless (i.e. no ASE beat, thermal, shot etc) system. In such a system for the times the crosstalk power is even fractionally bigger than the signal power, due to turbulence, there is a perfect detection of crosstalk resulting in a BER, for the signal, of 0.5. Equally, once the signal is bigger than the crosstalk, there is perfect signal detection with BER equal to 0. Thus, the error floor is simply given by $0.5 \times \text{prob}(\text{crosstalk power} > \text{signal power})$. This, under the assumption of equal long term average powers at the demux input, occurs for $h_d \leq L_{\text{demux},i}$ for turbulent signal with non-turbulent interferer, $h_i \geq 1/L_{\text{demux},i}$ for non-turbulent signal with turbulent interferer, and $h_i/h_d \geq 1/L_{\text{demux},i}$ for turbulent signal with turbulent interferer. The BER value where the error floors occur is thus determined by both the turbulence strength and the demux channel rejection (which directly controls the crosstalk power). Before the error floors occur, the system performance is limited by noise (ASE beat, thermal, shot etc.) and an increase in the signal-to-noise-ratio (SNR) of the system improves the BER. Similarly at low power, the noise dominates the signal and worsens the BER. However, in a noiseless system, the BER over the whole power range (e.g. in Fig. 3c) would be constant and equal to the BER value at which the system is limited by the combined effect of turbulence attenuation and crosstalk power.

The upstream and downstream required optical power at target BER of 10^{-6} is shown in Fig. 4 as a function of FSO link length and transmitter divergence angle for both OOK and DPPM systems. The interferer demux rejection is 35 dB and both interferer and signal are at the same distance from the remote node. The required optical power for the DPPM system is seen to be lower than that of the OOK system for all turbulent regimes considered. This result is consistent with the findings in the non-turbulent model which show that DPPM requires less power compared to OOK in a WDM free space system [25]. In Fig. 4a, the required optical power increases with the C_n^2 and FSO link length due to the perceived increase in turbulence strength as either or both parameters increases. This is not always the case, as will be seen and explained in later results. However, the increase in required optical power with respect to transmitter divergence angle and C_n^2 is a continuous trend owing to increase in beam spreading loss.

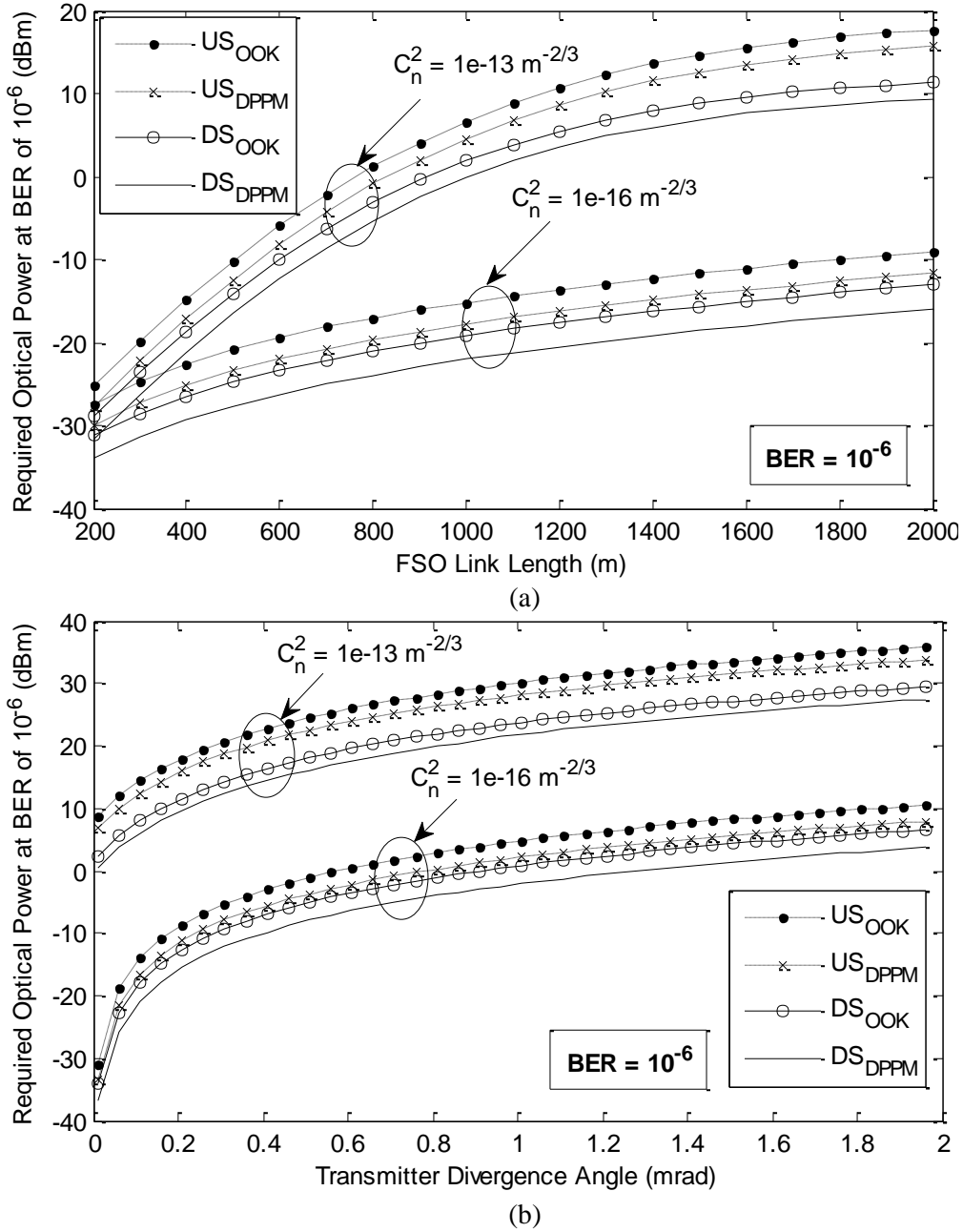


Fig. 4. Required Optical Power (dBm) for ST and WT at $L_{demux,i} = 35$ dB versus: (a) FSO Link Length (m), $\varphi_{TX} = 0.2$ mrad and (b) Transmitter Divergence Angle (mrad), $l_{fso} = 2000$ m

In Fig. 5, the required optical power for upstream transmission is considered for various interferer and signal FSO link length at target BER of 10^{-6} and demux rejection of 35 dB. The result in Fig. 5 is of the same form as previously obtained OOK results [12], and reveals that the effect of turbulence-accentuated crosstalk is worse when the interferer is closer to the

remote node compared to the desired signal. This is because the interfering signal experiences less loss on average and hence becomes stronger than the desired signal before the demux taken into account. Thus at certain interferer FSO link length, it is impossible to attain the target BER and an error floor occurs as seen in Fig. 5a. The target BER is achievable at reduced C_n^2 of $10^{-16} \text{ m}^{-2/3}$ value for every location within the FSO link length considered in Fig. 5b, with the required optical power rising as the position of the desired ONU moves away from the remote node. Therefore, it is highly important for a network designer to determine the closest distance to the remote node each ONU should be in order to obtain the required system performance with adequate consideration to the demux adjacent channel rejection ratio. For example, using a demux with adjacent rejection ratio of 35 dB as seen in Fig. 5a, when the interfering user is 500 m away from the remote node, then the desired ONU cannot be more than 1000 m away from the remote node for the target BER to be met at all turbulence regimes. To avoid some of these issues, a power control algorithm may be included in the system to monitor each ONU transmit power relative to the distance from the remote node and ensure that the same power is received at each user's receiver collecting lens as shown in the OOK model.

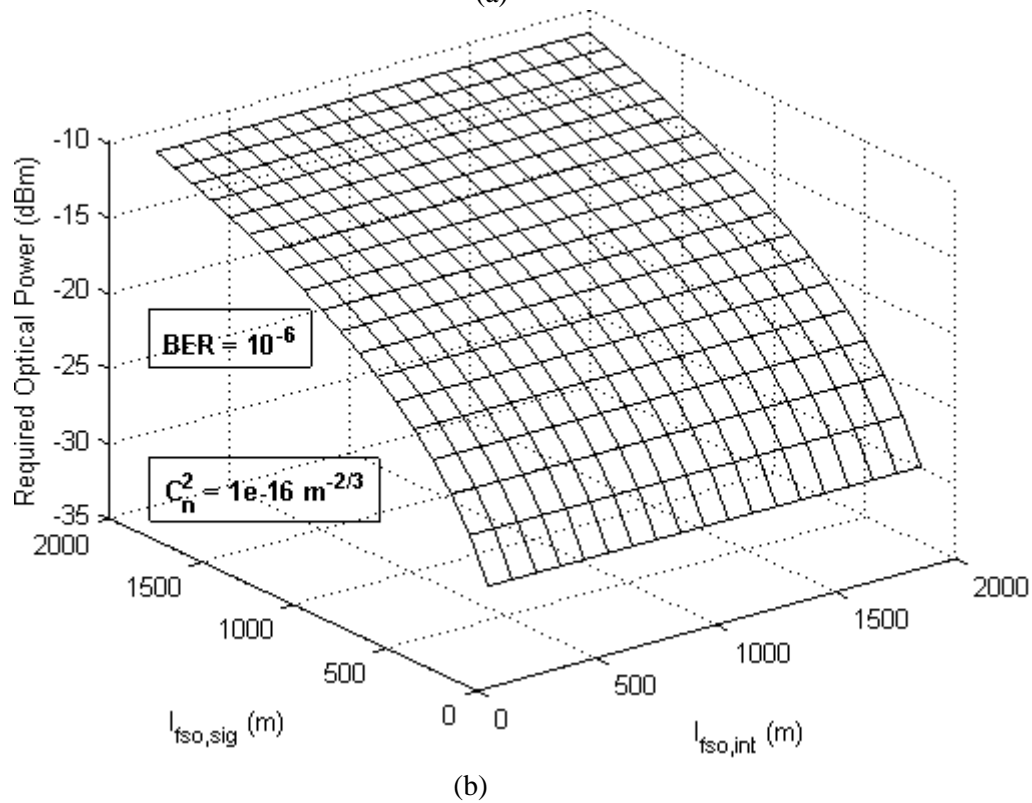
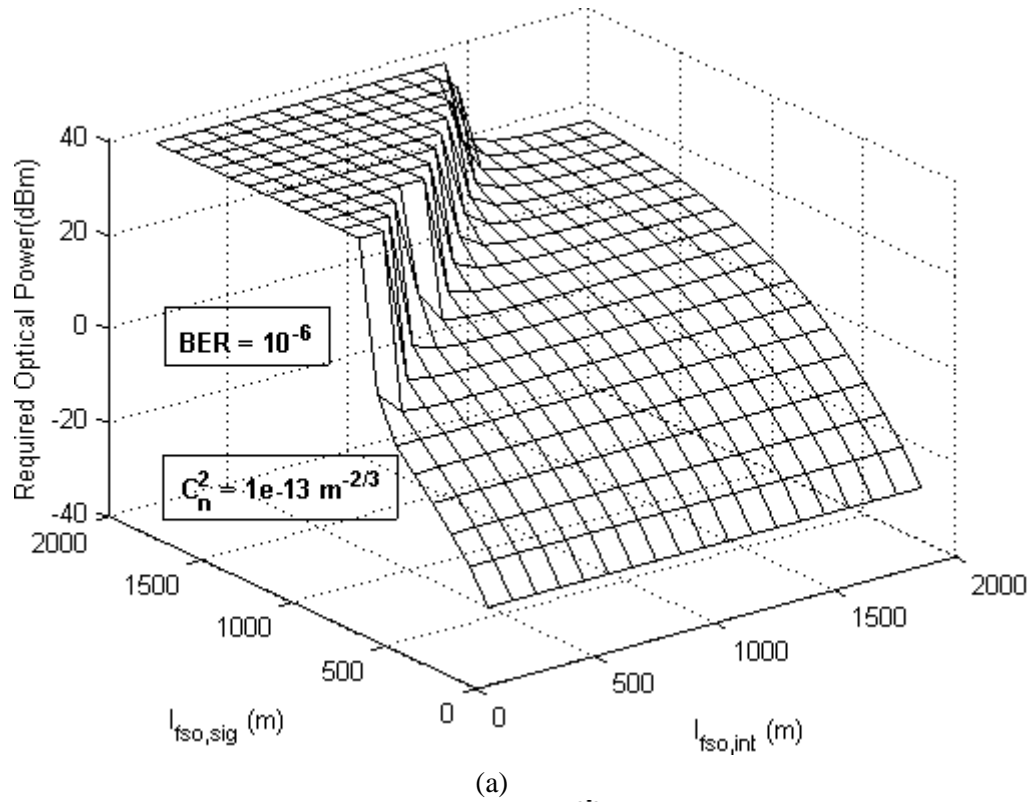


Fig. 5. Required Optical Power (dBm) for the upstream as a function of the FSO link lengths for signal and interferer (m) at $L_{\text{demux},i} = 35$ dB and target BER = 10^{-6}

In Fig. 6, the demultiplexer figure of merit in terms of adjacent channel rejection is considered for various interferers FSO link length at target BER of 10^{-6} and under different turbulence conditions. The FSO link length for the desired signal is fixed at 2000 m which is the maximum FSO link length considered in this work. It is clearly seen in Fig. 6a that if the desired ONU is positioned at 2000 m away from the remote node, then for another ONU (interferer) to be at 500 m to the remote node, a demux with adjacent rejection ratio greater than 45 dB is required so that the target BER is met for all turbulence regimes. Alternatively, the interfering user may be located at 1500 m from the remote node and a demux with 35 dB adjacent rejection ratio is used to meet the targeted BER performance. The target BER is easily achieved at weak turbulence condition as seen in Fig. 6b.

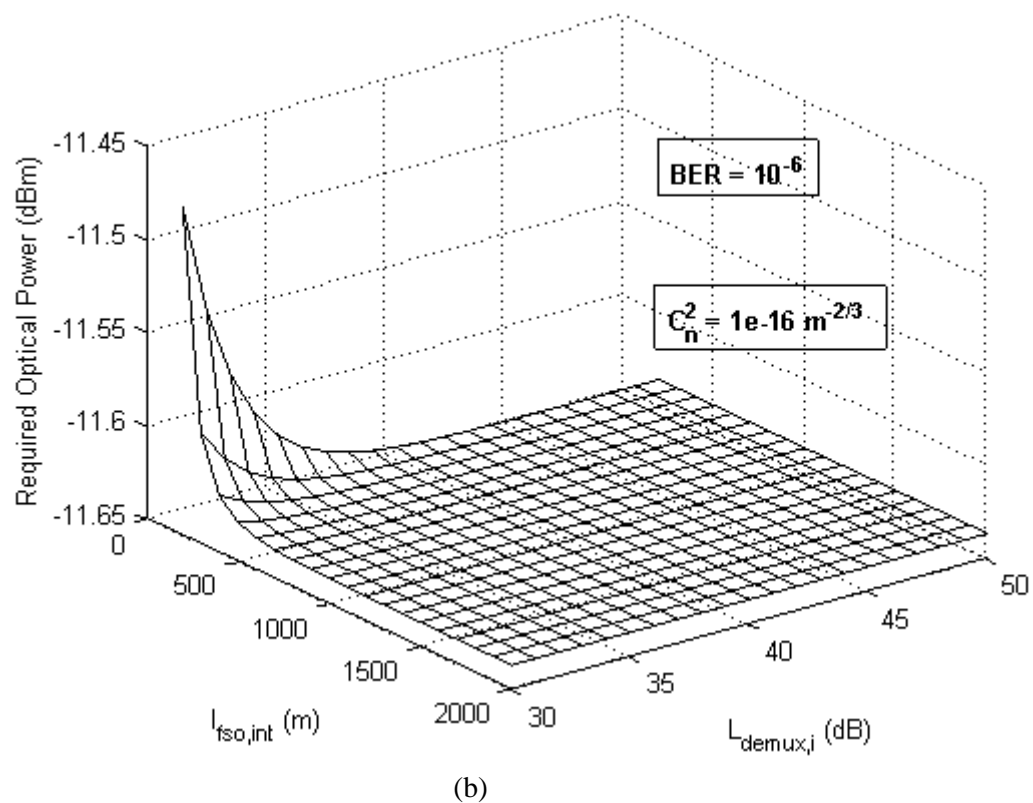
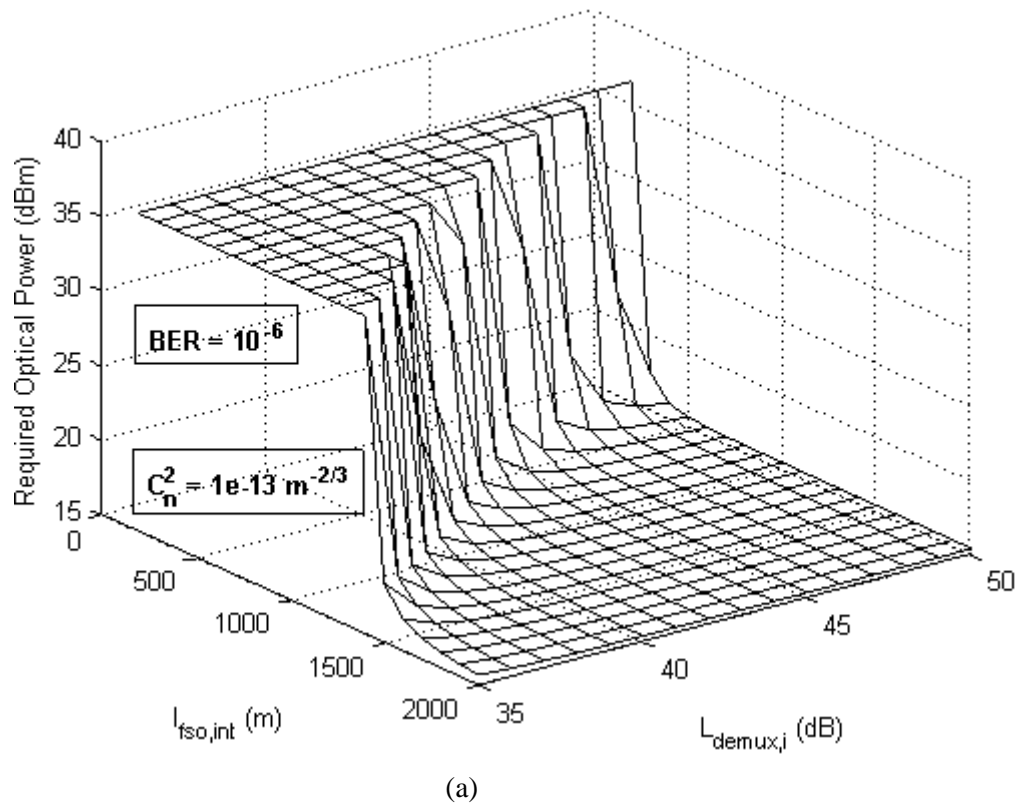
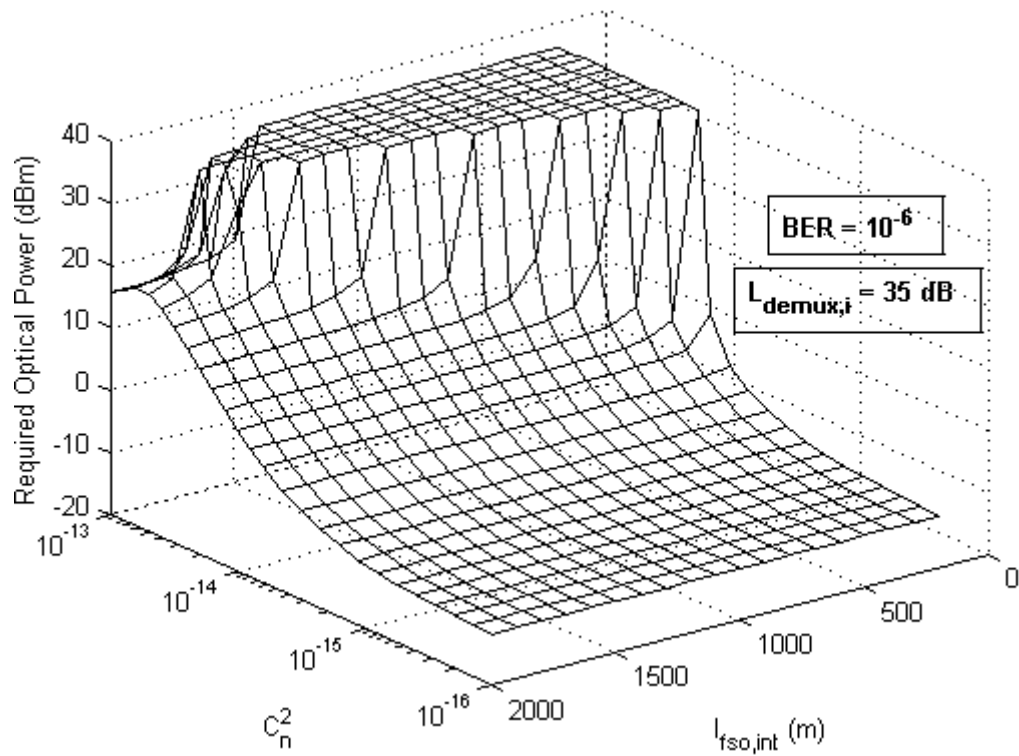


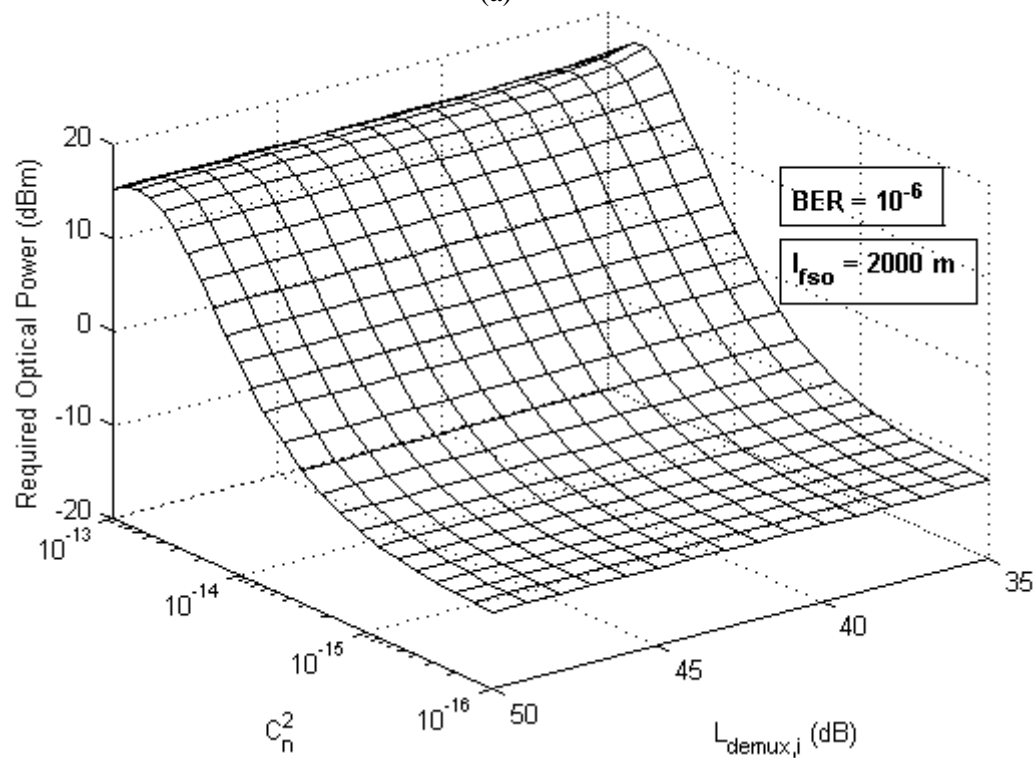
Fig. 6. Upstream Required Optical Power (dBm) as a function of demux channel rejection and interferer's FSO link (m) at $l_{\text{fso,sig}} = 2000$ m and target BER of 10^{-6}

The Rytov variance is related to scintillation index and is normally used for turbulence characterisation. It is directly related to the FSO link length and C_n^2 (see (2)) and gives an indication of the turbulence strength. Thus in Fig. 7, the required optical power for upstream transmission at target BER of 10^{-6} is examined for variable C_n^2 values and as a function of either FSO link length or demux loss (adjacent channel rejection). In Fig. 7a, error floor are seen gradually increasing as C_n^2 increases and/or interferer's distance from the remote node decreases, indicating positions where the target BER is not achievable. However, the floor disappears in Fig. 7b with both the desired signal and interferer permanently positioned at 2000 m from the remote node.

As noted before, the Rytov variance constantly increases with C_n^2 and FSO link length. However, It has been shown experimentally that the scintillation index and hence optical turbulence strength does not continuously increase with the Rytov variance [10, 40]. Generally, as the Rytov variance increases, the turbulence strength increases until a maximum is reached at a point referred to as the focusing regime [10] where the worst effect of random focusing is achieved. After this point, continued increase of the Rytov variance leads to loss of spatial coherence and a gradual decay in the scintillation index up to the saturated turbulence regime where it approaches unity [40]. This behaviour is responsible for the rise and fall in the required optical power along the C_n^2 axis in Fig. 7.



(a)



(b)

Fig. 7. Upstream Required Optical Power (dBm) as a function of the refractive index structure constant (C_n^2) at target BER = 10^{-6} : (a) $l_{fso,sig} = 2000$ m (b) $l_{fso,sig}$ and $l_{fso,int} = 2000$ m

The required optical power as a function of the interferer demux loss and refractive index structure constant for DPPM system is compared with OOK system in Fig. 8. The FSO link length for the signal and interferer are fixed at 1500 m so that the system operation is moved closer to the focusing regime for the C_n^2 values considered. It is seen that the DPPM system requires lower optical power compared to the OOK system for all values of C_n^2 and $L_{\text{demux},i}$ used in the analysis. In Fig. 8a, for target BER of 10^{-6} and $L_{\text{demux},i}$ of 35 dB, the single crosstalk effect is clearly seen worsening as the turbulence strength increases for both the OOK and DPPM systems. The system performance at different target BER values is examined for OOK and DPPM in Figs 8b and 8c. The result shows that for target BERs of 10^{-9} , 10^{-6} and 10^{-3} to be met at all turbulence regimes, the system requires demultiplexer with adjacent channel rejection greater or equal to 47 dB, 32 dB and 18 dB respectively. With forward error correction (FEC) implemented in most recent practical systems, operation at BER of 10^{-3} is becoming feasible and demultiplexers with 18 dB rejection is readily available.

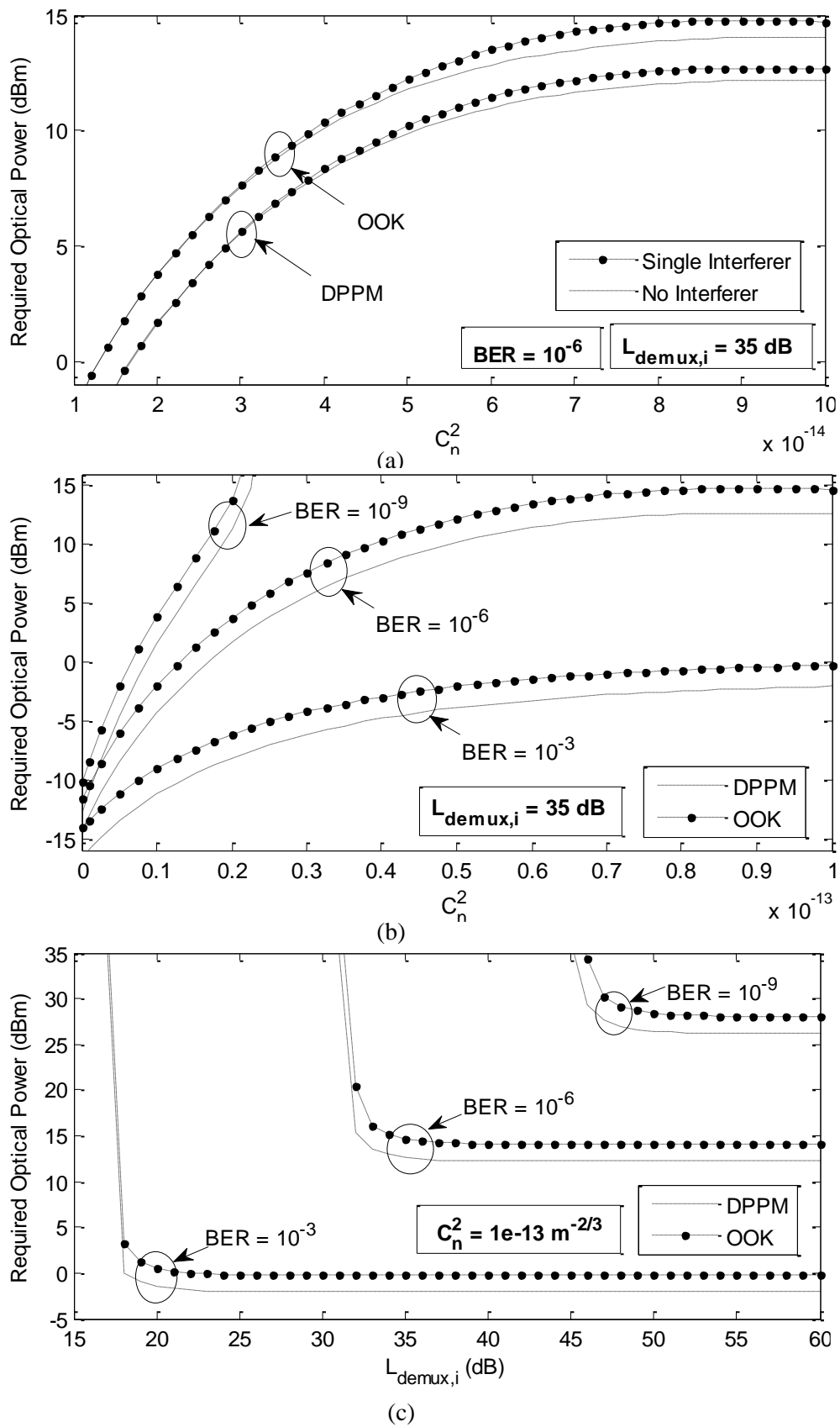
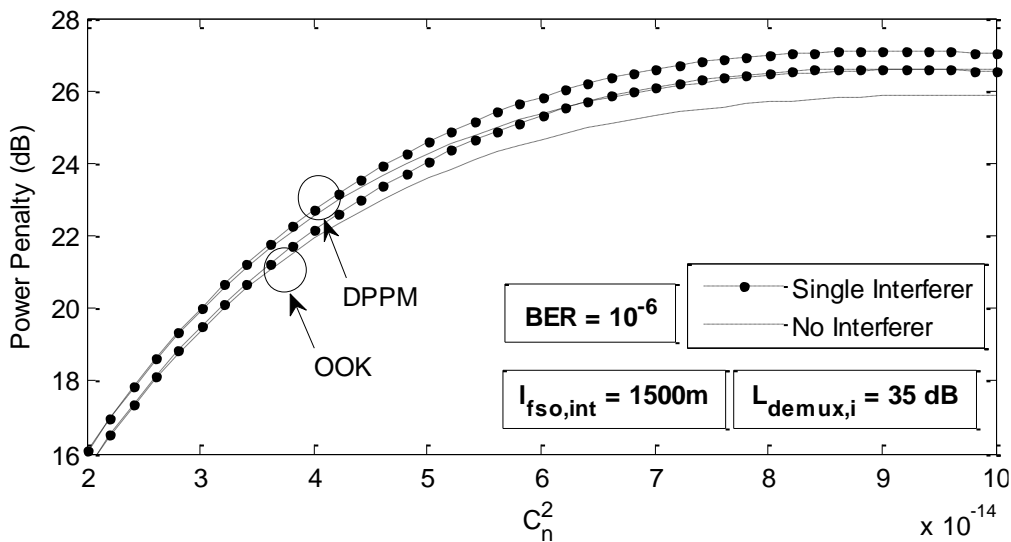
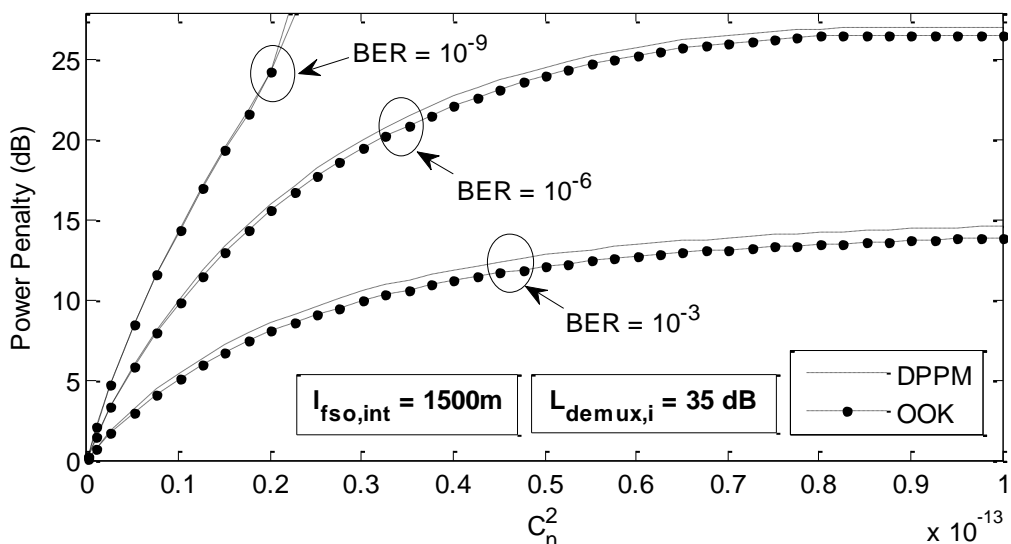


Fig. 8. Required Optical Power (dBm) for the upstream as a function of the refractive index structure constant (C_n^2) and interferer demux channel rejection at $l_{fso} = 1500$ m

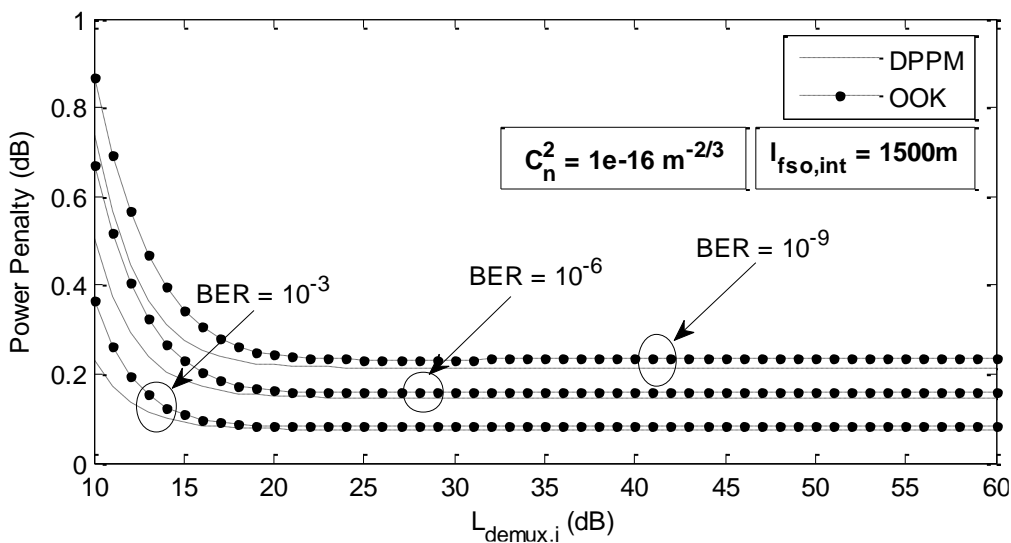
The power penalty results are shown in Fig. 9 for $l_{fs, sig} = 1500$ m. Unlike the non-turbulent WDM DPPM versus OOK crosstalk results in [25], Figs 9a and 9b indicate that the OOK system has slightly lower power penalty compared to the DPPM system under strong turbulence. As shown in Fig. 9a, with no interferer the DPPM power penalty is greater than the OOK power penalty by 0.2 dB, and increasing to 0.5 dB as the turbulence strength increases. This reduction in DPPM sensitivity over OOK systems in the presence of turbulence has been reported in [11], with no interferers. The difference between the power penalties of both systems is reduced in the presence of interferers (see Fig. 9a). And under no turbulence as seen in [25] or under weak turbulence as seen in Fig. 9c and 9d, the power penalty for the DPPM system tends to be lower than that of the OOK system. As shown in Fig. 9d, an interferer that is closer to the remote node causes more crosstalk to other users farther away, even at low c_n^2 value. Thus in the absence of power control, user positioning should be considered as an important design parameter.



(a)



(b)



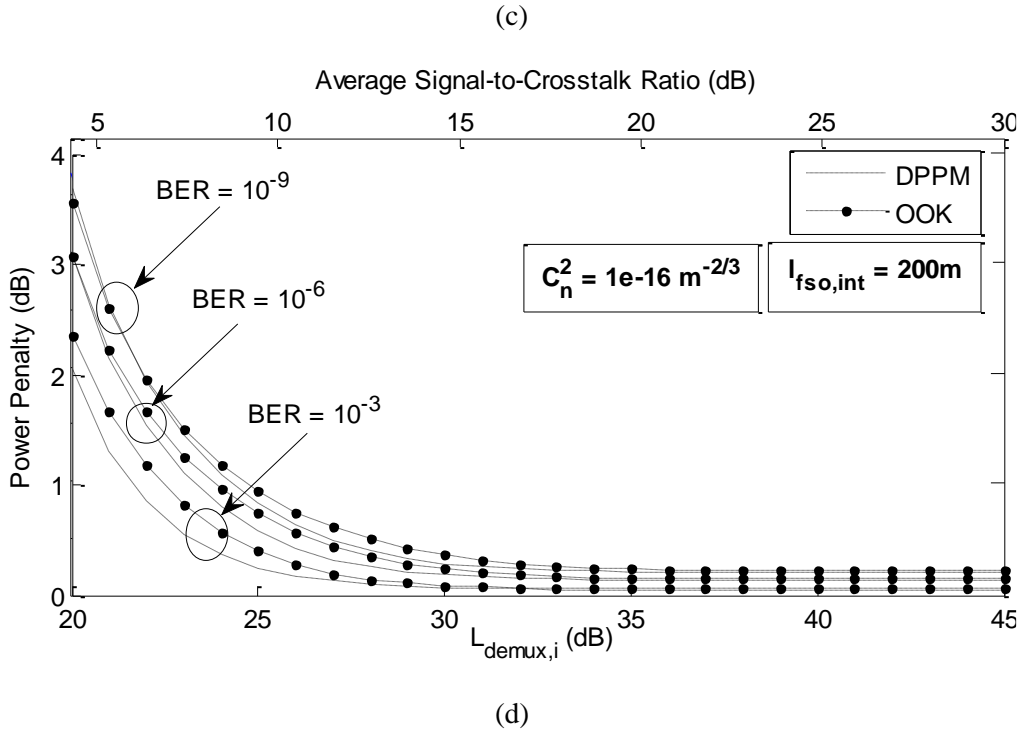


Fig. 9. Power penalty (dB) for the upstream as a function of the refractive index structure constant (C_n^2) and interferer demux channel rejection at $l_{fso,sig} = 1500$ m

7 Conclusion

The performance of a WDM DPPM system in the presence of turbulence-accentuated crosstalk is studied in this paper for the first time. Obtained results for required optical power and power penalties are compared with simple OOK NRZ system for a single crosstalk source. For all turbulence regimes, DPPM systems require lower optical power compared to OOK systems, but suffers a small loss in sensitivity as the turbulence strength increases. The existence of turbulence-accentuated crosstalk for the upstream transmission which somewhat restricts the relative distances between the remote node and both the interferer and the desired user for a specified target BER and demultiplexer adjacent rejection ratio is established in the results. Error floor occur in turbulent WDM DPPM systems with crosstalk and the relationship between the turbulence and the crosstalk at the onset of the error floor is shown in our analysis. Forward error correction (FEC) would benefit greatly the system in dealing with error floors and improving the achievable target BER as have been seen in other FSO systems.

References

1. Mukherjee, B.: 'WDM optical communication networks: progress and challenges'. *IEEE J. Selected Areas in Commun.*, 2000, **18**, (10), pp. 1810-1824
2. Ciaramella, E., Arimoto, Y., Contestabile, G., Presi, M., D'Errico, A., Guarino, V., Matsumoto, M.: '1.28 terabit/s (32x40 Gbit/s) wdm transmission system for free space optical communications'. *IEEE J. Selected Areas in Commun.*, 2009, **27**, (9), pp. 1639-1645
3. Forbes, M., Gourlay, J., Desmulliez, M.: 'Optically interconnected electronic chips: a tutorial and review of the technology'. *J. Electron. & Commun. Eng.*, 2001, **13**, (5), pp. 221-232
4. Forin, D. M., Beleffi, G. M. T., Curti, F., Corsi, N., De Sanctis, V., Sacchieri, V., Teixeira, A. J. L., et al.: 'On field test of a Wavelength Division Multiplexing Free Space Optics transmission at very high bit rates'. *9th Int. Conf. Telecommun.* 2007, pp. 77-80
5. Chang-Hee, L., Sorin, W. V., Byoung-Yoon, K.: 'Fiber to the Home Using a PON Infrastructure'. *J. Lightw. Technol.*, 2006, **24**, (12), pp. 4568-4583
6. Ramaswami, R., Sivarajan, K. N., Sasaki, G. H. *Optical Networks A Practical Perspective*. 3rd ed. Boston: Morgan Kaufmann Publishers; 2010.
7. Pei-Lin, C., Shenq-Tsong, C., Shuen-Te, J., Shu-Chuan, L., Han-Hsuan, L., Ho-Lin, T., Po-Hsuan, H., et al.: 'Demonstration of 16 channels 10 Gb/s WDM free space transmission over 2.16 km'. *Digest of the IEEE/LEOS Summer Topical Meetings* 2008, pp. 235-236
8. Aladeloba, A. O., Phillips, A. J., Woolfson, M. S.: 'Improved bit error rate evaluation for optically pre-amplified free-space optical communication systems in turbulent atmosphere'. *IET Optoelectron.*, 2012, **6**, (1), pp. 26-33
9. Qianling, C., Brandt-Pearce, M., Wilson, S. G.: 'Optically Amplified Wireless Infrared MISO Systems'. *IEEE Global Telecommun. Conf.*, 2007, pp. 4505-4510
10. Andrews, L. C., Phillips, R. L. *Laser Beam Propagation Through Random Media*. 2nd ed: SPIE Press, Bellingham, Washington; 2005.
11. Aladeloba, A. O., Phillips, A. J., Woolfson, M. S.: 'Performance evaluation of optically preamplified digital pulse position modulation turbulent free-space optical communication systems'. *IET Optoelectron.*, 2012, **6**, (1), pp. 66-74
12. Aladeloba, A. O., Woolfson, M. S., Phillips, A. J.: 'WDM FSO Network with Turbulence-Accentuated Interchannel Crosstalk'. *J. Opt. Commun. Netw.*, 2013, **5**, (6), pp. 641-651
13. Majumdar, A. K.: 'Free-space laser communication performance in the atmospheric channel'. *J. Opt. Fiber Commun. Rep.*, 2005, **2**, pp. 345 - 396
14. Ansari, N., Zhang, J. *Media Access Control and Resource Allocation for Next Generation Passive Optical Networks*: Springer; 2013.
15. Zuo, T. J., Phillips, A. J.: 'Performance of burst-mode receivers for optical digital pulse position modulation in passive optical network application'. *IET Optoelectron.*, 2009, **3**, (3), pp. 123-130
16. Kazovsky, L., Shing-Wa, W., Ayhan, T., Albeyoglu, K. M., Ribeiro, M. R. N., Shastri, A.: 'Hybrid Optical-Wireless Access Networks'. *Proc. IEEE*, 2012, **100**, (5), pp. 1197-1225
17. Liaw, S. K., Lai, Y. T., Chang, C. L., Shung, O.: 'AWG-based WDM-PON monitoring system using an optical switch and a WDM filter'. *Laser Phys.*, 2008, **18**, (9), pp. 1052-1055
18. Phillips, A. J., Cryan, R. A., Senior, J. M.: 'An optically preamplified intersatellite PPM receiver employing maximum likelihood detection'. *IEEE Photonics Technol. Lett.*, 1996, **8**, (5), pp. 691-693
19. Muhammad, S. S., Gappmair, W., Leitgeb, E.: 'PPM Channel Capacity Evaluation for Terrestrial FSO Links'. *Proc. Int. Workshop on Satellite and Space Commun.* 2006, pp. 222-226
20. Muhammad, S. S., Leitgeb, E., Koudelka, O.: 'Multilevel Modulation and Channel Codes for Terrestrial FSO links'. *2nd Int. Symp. on Wireless Commun. Syst.* 2005, pp. 795-799
21. Aldibbiat, N. M., Ghassemlooy, Z., McLaughlin, R.: 'Indoor optical wireless systems employing dual header pulse interval modulation (DH-PIM)'. *Int. J. Commun. Syst.*, 2005, **18**, (3), pp. 285-305
22. Ghassemlooy, Z., Popoola, W., Rajbhandari, S. *Optical Wireless Communications - System and Channel Modelling with MATLAB*. 1st ed. London: CRC Press; 2013.

23. Liu, L., Zhang, M., Liu, M., Zhang, X.: 'Experimental demonstration of RSOA-based WDM PON with PPM-encoded downstream signals'. *Chin. Opt. Lett.*, 2012, **10**, (7), pp. 070608
24. Caplan, D. O., Robinson, B. S.: 'WDM Mitigation of Nonlinear Impairments in Low-Duty-Cycle M-PPM Free-Space Optical Transmitters'. *Conf. Optical Fiber commun./National Fiber Optic Engineers Conf.*, 2008, pp. 1-3
25. Mbah, A. M., Walker, J. G., Phillips, A. J.: 'Performance evaluation of digital pulse position modulation for wavelength division multiplexing FSO systems impaired by interchannel crosstalk'. *IET Optoelectronics*, 2014, **8**, (6), pp. 245-255
26. Ohtsuki, T.: 'Performance analysis of atmospheric optical PPM CDMA systems'. *J. Lightw. Technol.*, 2003, **21**, (2), pp. 406-411
27. Bloom, S., Korevaar, E., Schuster, J., Willebrand, H.: 'Understanding the performance of free-space optics'. *J. Opt. Netw.*, 2003, **2**, (6),
28. Hai-Yin, H., Wan Chian, L., Hoa Le, M., Ghassemlooy, Z., Yi-Lin, Y., Shien-Kuei, L.: '2 x 80 Gbit/s DWDM Bidirectional Wavelength Reuse Optical Wireless Transmission'. *IEEE Photonics Journal*, 2013, **5**, (4), pp. 7901708-7901708
29. Khalighi, M., Schwartz, N., Aitamer, N., Bourennane, S.: 'Fading Reduction by Aperture Averaging and Spatial Diversity in Optical Wireless Systems'. *J. Opt. Commun. Netw.*, 2009, **1**, (6), pp. 580-593
30. Monroy, I. T., Tangdionga, E. *Crosstalk in WDM communication networks*. Norwell, Massachusetts, USA, : Kluwer Academic Publishers; 2002.
31. Dikmelik, Y., Davidson, F. M.: 'Fiber-coupling efficiency for free-space optical communication through atmospheric turbulence'. *Appl. Opt.*, 2005, **44**, (23), pp. 4946-4952
32. Ma, R., Zuo, T. J., Sujecki, S., Phillips, A. J.: 'Improved performance evaluation for DC-coupled burst mode reception in the presence of amplified spontaneous emission noise and interchannel crosstalk'. *IET Optoelectron.*, 2010, **4**, (3), pp. 121-132
33. 'Safety of laser products - part 1: Equipment classification, requirements and user's guide (Incorporating amendments A2:2001 and A1:2002)', (1994).
34. Sibley, M. J. *Optical Communications : components and systems*. 2nd ed. London: Macmillian Press Ltd; 1995.
35. Kiasaleh, K.: 'Performance of APD-based, PPM free-space optical communication systems in atmospheric turbulence'. *IEEE Trans. Commun.*, 2005, **53**, (9), pp. 1455-1461
36. Yu, C. X., Neilson, D. T.: 'Diffraction-grating-based (de)multiplexer using image plane transformations'. *IEEE J. Sel. Topics Quantum Electron.*, 2002, **8**, (6), pp. 1194-1201
37. Maru, K., Mizumoto, T., Uetsuka, H.: 'Demonstration of Flat-Passband Multi/Demultiplexer Using Multi-Input Arrayed Waveguide Grating Combined With Cascaded Mach-Zehnder Interferometers'. *J. Lightw. Technol.*, 2007, **25**, (8), pp. 2187-2197
38. Hirano, A., Miyamoto, Y., Kuwahara, S.: 'Performances of CSRZ-DPSK and RZ-DPSK in 43-Gbit/s/ch DWDM G.652 single-mode-fiber transmission'. *Optical Fiber Commun. Conf.*, 2003, pp. 454-456
39. Vetelino, F. S., Young, C., Andrews, L., Reolons, J.: 'Aperture averaging effects on the probability density of irradiance fluctuations in moderate-to-strong turbulence'. *Applied Optics*, 2007, **46**, (11), pp. 2099-2108
40. Andrews, L. C., Phillips, R. L., Hopen, C. Y. *Laser Beam Scintillation with Applications*: SPIE Press; 2001.